Propagation length of surface plasmons in a metal film with roughness

Andrei Kolomenski, Alexandre Kolomenskii,* John Noel, Siying Peng, and Hans Schuessler

Department of Physics, Texas A&M University, College Station, Texas 77843-4242

*Corresponding author: a-kolomenski@physics.tamu.edu

Received 6 May 2009; revised 2 September 2009; accepted 4 September 2009; posted 10 September 2009 (Doc. ID 110896); published 12 October 2009

The propagation of laser-excited surface plasmons along a gold film with surface roughness is directly observed via scattered light. The attenuation length of surface plasmons in a broad wavelength interval is calculated for smooth gold and silver films. The surface roughness, which was characterized with an AFM, introduces corrections to the attenuation length, angular dependence of the surface plasmon resonance, and the effective dielectric constant of the metal film. These corrections are also taken into account and discussed. © 2009 Optical Society of America

OCIS codes: 240.0310, 240.5770, 240.6680.

1. Introduction

Surface plasmons (SPs) are surface electromagnetic waves that can propagate along metal surfaces. In view of the superb dielectric properties of gold and silver, many studies were performed with these metals. The effects related to SPs were discovered more than a century ago, starting with reflection anomalies on gratings, observed by Wood [1], some of which were later explained in terms of surface plasmons, following Fano [2] and Ritchie [3]. Since the works of Kretschmann and Raether [4,5], the attenuated total internal reflection (ATIR) geometry, employing the matching of the phase velocities of the incident light and SPs along the metal surface (SP resonance condition) via a prism, is one of the most commonly used, and its different applications were reviewed by Raether [6]. Several new directions emerged more recently. The sensitivity of the propagation velocity of SPs to the dielectric properties of the adjacent medium makes them an efficient tool in biosensing [7]. The attenuation of SPs determines the width of the SP resonance, which affects the sensitivity of the sensor. The attenuation length of SPs also determines the spatial resolution of an imaging technique in the ATIR configuration [8]. A planar optical geometry is attractive for compact optical devices interconnected with electronic components, therefore the development of the optics of SPs [9] is also one of the promising directions of research. It was shown that, for a symmetrical structure with the metal film sandwiched between two dielectric layers, a mode of long-range SPs can propagate [10]. In view of the special requirements of the geometry of such a system, long-range plasmons are not considered in this paper.

For the above-mentioned developments, the propagation of the SPs is crucial, and it was studied using different approaches. The attenuation of SPs is related to the angular width of the minimum in the reflected light, and it strongly depends on the light wavelength [4,5]. The portion of light converted into SPs eventually produces heat. Consequently, SP resonance can be studied with photo-acoustic techniques [11]. When excited with white light, SPs of different frequencies propagate different distances giving rise to "color jets" that can be viewed in a microscope [12]. Propagating SPs can be visualized due to effects of their near field. For instance, when the medium adjacent to the metal film is fluorescent, a decaying trace of fluorescence can be observed along

0003-6935/09/305683-09$15.00/0

the direction of SPs propagation [13]. Also other optical near-field techniques have been developed, such as the photon scanning tunneling microscope, which relies on the near-field coupling of the SP field to the sharpened optical fiber tip of a probe [14].

The attenuation length is affected by the scattering of SPs on the surface roughness, scratches, and inhomogeneities of the metal film or the adjacent medium [15,16]. Much work was dedicated to investigating the possibility of extracting roughness parameters from measurements of the scattered light [17,18] and relating them with the observed SP resonance angular dependences [19]. The absorption of the adjacent medium provides additional attenuation, and this effect can be used to measure its absorption [20,21].

In the present work, we directly observe the propagation of SPs on a gold film with roughness by detecting the scattered light in the far field with a microscope and an attached CCD camera. The experimental results are compared with model calculations that take into account different factors affecting attenuation, including surface roughness. The experimental study was performed at two optical wavelengths for 633 and 805 nm. For reference, the calculations of the SP attenuation length were performed in a broad wavelength interval.

2. Theoretical Description

The attenuation length of SPs in a planar system consisting of an arbitrary number of smooth layers (without roughness), some of which are metallic for guiding SPs, can be found with the following procedure that is based on the expressions for the intensity reflection coefficient, or reflectivity for short, R. The problem of reflection of light from a layered system leads to a system of algebraic equations. For a given frequency the complex wavenumber of a SP corresponds to the zero of the determinant of this system. Consequently, the solution for zero of the denominator of the reflection coefficient, or the requirement $|R| \to \infty$, determines the dispersion equation of SPs [5,22]. For a multilayered structure, the reflection coefficient can be determined following the iterative procedures [23] (described below) and [22] (the latter is a generalization of the approach used in [5]). The dispersion relation was also derived explicitly for an arbitrary number of layers [24], and for a four layer system an explicit form of the determinant is presented in [25]. Thus, knowing $R = R(k, \omega)$ as a function of the parallel to the interface wave vector component, k, and the light frequency, ω, one can find the dispersion relation of SPs by solving the equation $|R^{-1}| = 0$.

We calculated the reflectivity R for a layered system with smooth planar interfaces and an arbitrary number M of layers using recursive equations [23]:

$$R = \left| \frac{Z_{\text{in},1} - Z_0}{Z_{\text{in},1} + Z_0} \right|^2. \qquad (1)$$

In this recursive procedure for an intermediate layer m, each input impedance $Z_{\text{in},m}$, as well as each layer impedance Z_m, are calculated in descending sequence of layer numbers. It is assumed that the two outer media are semi-infinite, and the medium $m = 0$ corresponds to $z > 0$. The laser beam is incident on plane $z = 0$ at an angle θ with respect to the positive z direction, which also coincides with the direction of the normal to the interface. The input impedance and layer impedance at a particular layer m are calculated from the relations

$$Z_{\text{in},m} = Zm \left[\frac{Z_{\text{in},m+1} - iZ_m \tan(k_{m,z} d_m)}{Z_m - iZ_{\text{in},m+1} \tan(k_{m,z} d_m)} \right], \qquad (2)$$

where $Z_m = k_{m,z}/(\varepsilon_m k_0)$, $Z_{\text{in},M-1} = Z_{M-1}$, $k_{m,z} = \sqrt{\varepsilon_m k_0^2 - k^2}$, $k = k_0 \sqrt{\varepsilon_0} \sin\theta$, $k_0 = 2\pi/\lambda_0$, λ_0 is the light wavelength in vacuum, i is the imaginary unit, and the integer index m runs from 0 to $M - 1$. The field in each medium can be presented as a sum of a direct wave $\propto \exp(-ik_{m,z}z)$ and (except for the last medium with $m = M - 1$) a backward wave $\propto \exp(ik_{m,z}z)$, propagating correspondingly into $(-z)$ and $(+z)$ directions. Consequently, the requirement $\text{Im}(k_{m,z}) \geq 0$ must be fulfilled for these waves to have finite amplitudes.

The condition $|R^{-1}| = 0$ gives an equation for k, which in general has a complex solution $k_{\text{SP}}(\omega)$. Although k_{SP} enters the denominator of Eq. (1) in the same way as k, it has a different meaning. We introduced k as a projection of the wave vector of the incident light on the metal surface boundary. For the solution k_{SP}, its real part determines the wavenumber, and its imaginary part determines the amplitude attenuation coefficient of the SP. The resonance excitation corresponds to the condition $k = \text{Re}(k_{\text{SP}})$, which takes place at the incidence angle of the reflectivity minimum that also corresponds to the maximum conversion of light into SPs.

To take into account the influence of the surface roughness on the propagation of SPs, we examined a three layer system consisting of a glass prism ($m = 0$), a metal film ($m = 1$) with a complex dielectric permittivity $\varepsilon_1 = \varepsilon_{1,r} + \varepsilon_{1,i}$ and a thickness d_1, and an adjacent dielectric medium ($m = 2$), which in general can also have losses, so that $\varepsilon_2 = \varepsilon_{2,r} + i\varepsilon_{2,i}$. We assume that the metal film at the interface with the medium $m = 2$ has certain roughness, and then refer to the models that neglect roughness as "0-order models". The presence of roughness will be taken into account in the first order perturbation approach; see further Eqs. (8) and (13).

In the approximation $\varepsilon_{1,r} \gg \varepsilon_{1,i}$ and $\varepsilon_{2,r} \gg \varepsilon_{2,i}$, which is usually fulfilled for gold and silver films in the optical and IR spectral regions, the reflectivity can be expressed [5] in a form with Lorentzian denominator, explicitly showing the resonance character of the interaction:

$$R = 1 - \frac{4(\Gamma_i + \Gamma_r)\Gamma_{\mathrm{rad}}}{(k - k_{\mathrm{SP},r})(k - k_{\mathrm{SP},r}^{*})}, \tag{3}$$

where

$$\begin{aligned} k_{\mathrm{SP},r} &= k_{\mathrm{SP}} + (\Delta k_r + i\Gamma_r) \\ &= k_p + \Delta k_p + \Delta k_r + i(\Gamma_i + \Gamma_{\mathrm{rad}} + \Gamma_r) \end{aligned} \tag{4}$$

is the complex wavenumber of the SP that takes into account surface roughness. The star $(*)$ denotes complex conjugation, $\Gamma_i = \Gamma_{i1} + \Gamma_{i2}$; $k_p = (2\pi\, n_p/\lambda_0)$ is the wavenumber of the SP corresponding to the case of infinitely thick metal film, and $\Delta k_p = [(a^2 - {\varepsilon_0}^2)/(a^2 + {\varepsilon_0}^2)]g$ is the correction to this number accounting for the finite thickness of the film. The following notations were introduced in the above formulas:

$$\begin{aligned} g &= 2k_p {n_p}^2 \exp[-2k_p(\varepsilon_{1r}/\varepsilon_{2r})^{1/2} d_1]/(\mathrm{Re}\varepsilon_{2r} + |\varepsilon_{1r}|), \\ a &= |\varepsilon_{1r}|(\varepsilon_0 - \varepsilon_{2r}) - \varepsilon_0\varepsilon_{2r}, \\ n_p &= [\varepsilon_{1r}\varepsilon_{2r}/(\varepsilon_{1r} + \varepsilon_{2r})]^{1/2}, \\ \Gamma_{i1} &= k_p(\varepsilon_{1i}/2{\varepsilon_{1r}}^2){n_p}^2, \\ \Gamma_{i2} &= k_p(\varepsilon_{2i}/2{\varepsilon_{2r}}^2){n_p}^2, \\ \Gamma_{\mathrm{rad}} &= [2a\varepsilon_0/(a^2 + {\varepsilon_0}^2)]g. \end{aligned} \tag{5}$$

The quantities Γ_{i1} and Γ_{i2} describe the damping that originates from the internal losses in the metal and the adjacent medium, respectively, and Γ_{rad} describes the radiative loss due to the transmission of light through the metal film. Quantities Δk_r and Γ_r in Eq. (4) describe the changes of the real and imaginary part of the wavenumber due to surface roughness. The term Γ_r includes additional contributions to attenuation of SPs related to the changes of the dielectric properties due to the surface roughness, rescattering losses, as well as the losses resulting from the conversion of SPs into radiative bulk waves.

The SP resonance is most pronounced for the optimal metal film thickness $d_{1,\mathrm{opt}}$, which is about 47 nm for gold. The inverse of the imaginary part of $k_{\mathrm{SP},r}$ determines the attenuation length (at e^{-1} level) of the SPs in terms of the SP field amplitude. However, the decay of the SP intensity, which is proportional to the square of the field, is measured in most experiments. As a result, for the intensity attenuation length a factor of 0.5 must be introduced:

$$L_{\mathrm{sp},r} = 0.5(\Gamma_{i1} + \Gamma_{i2} + \Gamma_r + \Gamma_{\mathrm{rad}})^{-1}. \tag{6}$$

As it follows from Eq. (3), this length can also be approximately determined from the FWHM width $\Delta\theta$ of the resonance curve:

$$L_{\mathrm{sp}} \approx (\sqrt{\varepsilon_0}k_0 \cos\theta_{\mathrm{res}}\Delta\theta)^{-1}. \tag{7}$$

The incident light with a power P_0 scatters from a rough surface on the back side of the metal film yielding the power dP that goes into a solid angle element $d\Omega$ [17]:

$$dP = 4P_0\left(\frac{\pi}{\lambda}\right)^4 \frac{|\varepsilon_2|^{0.5}}{\cos\theta}|t_{012}(\theta)|^2|W(\theta)|^2\tilde{G}(\mathbf{k}' - \mathbf{k})d\Omega\ , \tag{8}$$

where θ_0 is the incidence angle of the excitation light, $|t_{012}(\theta)|^2$ is the transmission function for a two-boundary system with a metal film [specifically, this function is the square of the ratio of strengths of the magnetic field at the second boundary (metal-air) and in the incident wave]. $|W(\theta)|^2$ is the dipole radiation function of the surface (for an explicit expression see [17], Eq. (2)). $\tilde{G}(\mathbf{k})$ is the two-dimensional power spectral density (PSD) function

$$\tilde{G}(\mathbf{k}) = \frac{1}{(2\pi)^2}\int G(\mathbf{r})\exp(-i\mathbf{k}\mathbf{r})\mathrm{d}\mathbf{r} \tag{9}$$

of the correlation function of the surface roughness $\varsigma(\mathbf{r})$:

$$G(\mathbf{r}) = \frac{1}{S}\int_S \varsigma(\mathbf{r}')\varsigma(\mathbf{r}' + \mathbf{r})\mathrm{d}\mathbf{r}', \tag{10}$$

where the integral is taken over the illuminated area of the rough surface S. In Eq. (8) the argument of the PSD function is the difference of the interface components of the wave vectors of the scattered and incident light. We assume, following the often used approximation, that the roughness correlation function is isotropic and Gaussian, i.e.,

$$G(\mathbf{r}) = \delta^2 \exp\left(-\frac{r^2}{\sigma^2}\right), \tag{11}$$

where σ is the correlation length and δ is the average height of the roughness. In this particular case, the two-dimensional PSD function is proportional to the one-dimensional PSD function, $\tilde{G}_1(k)$, namely

$$\tilde{G}(k) = \frac{\sigma}{2\sqrt{\pi}}\tilde{G}_1(k), \qquad \tilde{G}_1(k) = \frac{\delta^2\sigma}{2\sqrt{\pi}}\exp\left(-\frac{k^2\sigma^2}{4}\right). \tag{12}$$

The roughness changes the complex wavenumber of SPs as well as the SP dispersion equation [26–29]. We calculated this wavenumber change due to roughness

$$\Delta k_{\mathrm{SP}} = k_{\mathrm{SP},r} - k_{\mathrm{SP}} = \Delta k_r + i\Gamma_r, \tag{13}$$

using Eq. (A42) of [29]. The real part of Δk is responsible for the angular displacement of the SP resonance and the imaginary part determines the

change in attenuation of SPs and also the change of the width of the resonance curve due to roughness. Using the approximation of Eqs. (4) and (5), one can also calculate an *effective dielectric constant* of the metal, $\varepsilon_{1,\mathrm{eff}}$, which gives the same change Δk_{SP} as the surface roughness (assuming that its contribution is relatively small), i.e., $\varepsilon_{1,\mathrm{eff}}$ can be found from the equation

$$[k_p + \Delta k_p + i(\Gamma_i + \Gamma_{\mathrm{rad}})]|_{\varepsilon_1 -> \varepsilon_{1,\mathrm{eff}}} = [k_p + \Delta k_p + \Delta k_r + i(\Gamma_i + \Gamma_r + \Gamma_{\mathrm{rad}})]|_{\varepsilon_1}. \quad (14)$$

In the left-hand side of this equation ε_1 is substituted by $\varepsilon_{1,\mathrm{eff}}$, while the right-hand side is calculated for ε_1, and it takes into account the corrections Δk_r and Γ_r due to roughness. The obtained value of $\varepsilon_{1,\mathrm{eff}}$ can then be used to calculate the modified-by-roughness SPR curve, using the exact formulas of Eqs. (1) and (2) or the approximate expressions of Eqs. (3)–(5). The results of such calculations are presented in Section 4.

The transmission function is determined as [6]

$$|t_{012}(\theta)|^2 = \left|\frac{(1 + r_{21})(1 + r_{10})\exp(ik_1 d_1)}{1 + r_{21} r_{10}\exp(2ik_1 d_1)}\right|^2, \quad (15)$$

where $r_{ij} = (\varepsilon_j k_i - \varepsilon_i k_j)/(\varepsilon_j k_i + \varepsilon_i k_j)$ with $i = 1, j = 0$ and $i = 2, j = 1$ are the Fresnel's reflection coefficients at two interfaces for p-polarized light. For such light the function $|t_{012}(\theta)|^2$ has a resonance character, and it strongly increases at $\vartheta \approx \vartheta_{\mathrm{SPR}}$, acquiring its maximum in proximity of the optimal thickness of the metal film. Thus, the intensity of the scattered light can be strongly enhanced at the SP resonance.

In the experiment, we inferred the attenuation length of SPs from the decay of the scattered light intensity with the distance from the illumination stripe. To evaluate this attenuation length we used the following procedure. We assume that the laser beam with a power P is focused on the surface in a stripe with a Gaussian intensity distribution $I(x,y) = (P/\pi ab)\exp(-x^2/a^2 - y^2/b^2)$, where b and a are the length and the width, respectively. For a typical attenuation length of surface plasmons L_p, the dimensionless diffraction parameter $(\lambda_p L_p/\pi b^2)$ is small, where λ_p is the wavelength of the SPs; thus the propagation of surface plasmons from a strip can be considered one dimensional. We assume that, on average, the surface roughness is uniform along the film, and consequently the scattering of SPs into radiative bulk waves is, on average, the same over the surface. At the SP resonance, light due to scattering of SPs prevails over the scattering produced by the directly incident light because of the enhancement factor of Eq. (15) for the SP field. The SP intensity at a certain position x is proportional to the integral of all partial contributions from different cross sections of the irradiation spot, taking into account also the decay of SPs during their propagation. Then the observed density F of the light radiation from the surface in the far field is proportional to the integral

$$F(x) \propto \exp(-x^2/a^2)\int_0^\infty \exp[-x_1^2/a^2 \pm x_1(2x/a^2 + 1/L_{\mathrm{sp}})]\mathrm{d}x_1, \quad (16)$$

representing the intensity distribution of the SP field along the surface, where signs $(\pm)$ correspond to the SPs propagating in the directions $x \to \mp\infty$. For large distances, $|x| \gg a$, Eq. (16) reduces to an exponential decay $\propto \exp(\pm x/L_{\mathrm{sp}})$. The distribution of Eq. (16) has asymmetry, because for the ATIR configuration SPs propagate on the surface in the direction of the projection of the wave vector of the incident light on the interface plane. In the following, Eq. (16) and its asymptotic exponential function is used for fitting and extraction of the SP attenuation length from measurements of the distribution of the scattered light.

3. Experimental Setup

To excite and observe SPs and their propagation properties the following setup was employed (Fig. 1). For the excitation we used the Kretschmann–Raether configuration, with a prism enabling the coupling of the incident laser light to the surface plasmon mode [5,6]. Two different lasers were utilized for the excitation of SPs at two different wavelengths: a He–Ne laser with a power of 3 mW and a wavelength of 633 nm and a cw Ti:sapphire laser with a wavelength of 805 nm and a power attenuated to about 20 mW. For comparison, the measurements were done for p and s polarizations of the incident light. For this purpose, the initial polarization of the beam was adjusted with a half-wave plate, so that the intensities of the p and s components of the incident light were of the same order of magnitude.

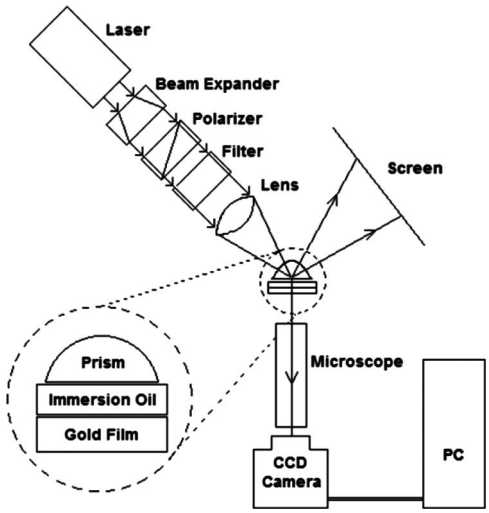

Fig. 1. Experimental setup for studies of surface plasmons.

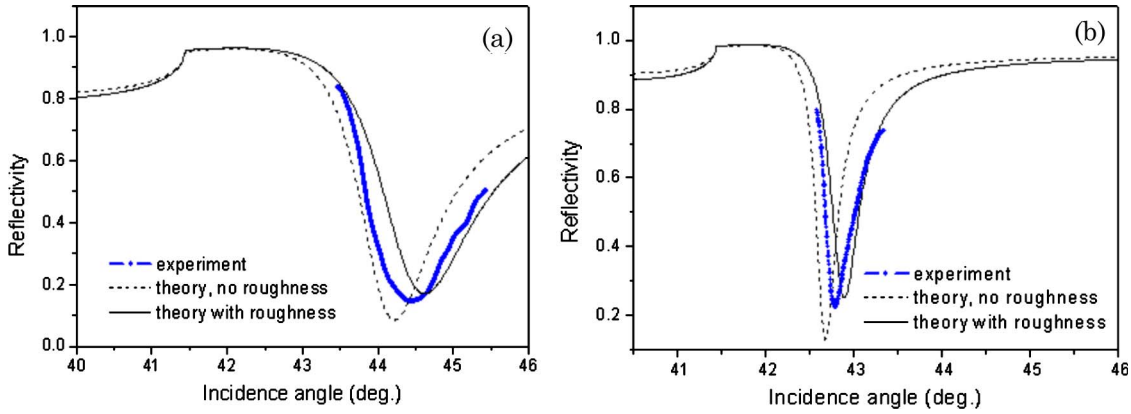

Fig. 2. (Color online) Measured and calculated SPR curves for (a) 633 nm and (b) 805 nm.

The laser beam was initially expanded with a collimator to a 10 mm diameter and then focused with a cylindrical lens through a hemicylindrical prism into a stripe of about 8 μm width on the surface of a sensor chip (research grade CM5 chip, BIAcore AB). The sensor chip had a 47 nm thick gold film on a 0.3 mm thick slide of BK7 glass. The carboxymethyl dextran layer was removed from the surface of the film, which was roughened in the process. The light passing through the prism was coupled to the clear side of the glass slide by using a matching fluid (Cargille Labs Incorporated). The SP resonance excitation took place when the light was p polarized (with a calcite polarizer, $p-s$ intensity ratio $10^5:1$). The light scattered by propagating SPs close to the normal direction on the back side of the gold film (opposite to the side of the incident laser beam) was collected by a microscope (30× magnification) and detected with a CCD camera. To avoid saturation of the CCD camera, the light intensity was adjusted by neutral density filters. The imaged surface region encompassed the area around the strip illuminated by the focused laser beam. The CCD image was formed by 2048 × 1500 pixels, and a typical acquisition time was about 60 μs. The resulting digitized 2D image reflected the distribution of the intensity of scattered light over the surface. The SP resonance phenomenon manifested itself as a dark area in the reflected beam projected on the screen. To register the intensity distribution of the reflected light, the CCD camera was appropriately positioned in place of the screen. From the CCD camera the image was transferred to a PC for further processing with XCAP software (EPIX Incorporated). Roghness measurements of the gold film were done using tapping mode AFM (Veeco, CP II) in ambient air at driving frequencies ranging from 70–90 kHz. Antimony-doped silicon cantilevers with a spring constant of 15 N/m and nominal tip radius of 8 nm were used.

4. Results

The angular distribution of the reflected light intensity in the vicinity of the SPR angle for 633 and 805 nm is shown in Fig. 2. The minima indicate the angular positions of the SP resonance, which occurred at the light incidence angle onto the gold film interface of 44.5° for 633 nm and 42.8° for 805 nm. The dashed lines show calculated SPR curves without surface roughness. Thin solid curves are obtained taking into account roughness correction [Eq. (13)], then calculating the value of the effective dielectric constant $\varepsilon_{1,\mathrm{eff}}$ from Eq. (14) and substituting it into the formulas of Eqs. (1) and (2). For the calculations we used the dielectric constants compiled in Table 1. The roughness parameters were determined from measurements with an AFM; see Fig. 3(a). From the profile measurements, the 1D PSD function of the surface roughness was calculated Fig. 3(b). By fitting the 1D PSD function with a Gaussian of the form of Eq. (12) [see the inset in Fig. 3(b)], we determined $\delta = 2.0$ nm and $\sigma = 36$ nm.

The plots of the decay of the light intensity away from the focal region are shown in Fig. 4 for the excitation by both p and s polarizations. The light intensity decays from the center of the excited SPR stripe.

Table 1. Dielectric Constants of Gold ε_1 and Glass ε_2, SP Attenuation Length Without Roughness L_{sp}; Effective Dielectric Constant $\varepsilon_{1,\mathrm{eff}}$; Attenuation Length $L_{\mathrm{sp},r}$ Calculated with Roughness ($\delta = 2.0$ nm, $\sigma = 36$ nm) and Experimentally Determined SP Attenuation Lengths

λ (nm)	ε_1	ε_2	$L_{\mathrm{sp}}(\mu\mathrm{m})$	$\varepsilon_{1,\mathrm{eff}}$	$L_{\mathrm{sp},r}$ (m)	L_{sp} Experiment (μm)
633	$-10.8+0.76i$ [30]	2.30	4.4	$-9.6+0.62i$	3.6	3.0 [Fig. 2(a)]
	$-11.0+1.5i$ [31]		3.7	$-8.6+0.88i$	2.5	3.4 [Fig. 4(a)]
	$-9.1+1.0i$ [32]		2.7	$-8.2+0.85i$	2.3	
805	$-23.0+0.75i$ [30]	2.28	23	$-20.1+0.60i$	17	17 [Fig. 2(a)]
	$-22.3+2.0i$ [31]		14	$-19.6+1.7i$	11	15 [Fig. 4(b)]
	$-26.8+1.8i$ [32]		24	$-22.6+1.3i$	18	

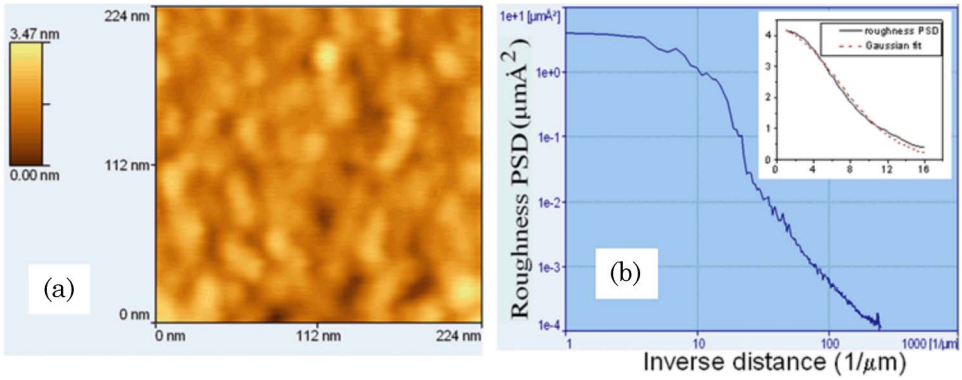

Fig. 3. (Color online) Surface roughness measured with AFM: (a) false color surface relief and (b) the PSD function of the surface roughness in logarithmic scale. The inset shows the fitting of the PSD function by $\tilde{G}_1(k)$ of Eq. (12) with $\delta = 2.0$ nm and $\sigma = 36$ nm [axes have the same units as in Fig. 3(b)].

The small peaks in Fig. 4(b) appearing on the slope of the dependences originate from scattering on scratches and on local inhomogeneities of the gold film. For coupling with a prism, as in our case, the SPs propagate in the same direction as the projection of the wave vector of the incident light on the surface. Consequently, the light intensity falls off on a relatively long distance along the direction of the SP propagation (negative x direction in Fig. 5) and on a shorter distance in the positive x direction.

The attenuation length is determined from the decaying tail in the distribution of the scattered intensity beyond the laser illumination stripe on the surface of the gold film. Fitting the curve for p polarization of Fig. 4(a) with Eq. (16) was performed for the whole range presented. For Fig. 4(b), the fitting was done only in the range shown by the fitting curve, since the presence of a flat portion shows a saturation of the CCD camera close to the excitation stripe.

As the result of fitting, we found the following parameters for the optical wavelength 633 nm: width $a = 4\,\mu$m and the attenuation length $L_{sp} = 3\,\mu$m. For 805 nm, the fitting produced the value $L_{sp} = 15\,\mu$m. The large (by a factor of about 20) difference in the intensity of the images produced by p and s polarizations is due to the fact that SPs are excited only for p-polarized light. Consequently, on the back side of the gold film, where the scattered light is registered, for p polarization the scattering is enhanced by the factor of Eq. (15). To illustrate the effect of this enhancement, the factor $|t_{012}(\theta)|^2$ was calculated and plotted in Fig. 5 for the parameters of our system and the dielectric constants of gold at 633 nm and 805 nm (solid lines). Dashed lines show similar calculations performed for the determined effective dielectric constants, accounting for the roughness of the film. It should be noted that the experimental enhancement factor is somewhat less, because it was observed for a convergent incident wave, while the calculation was performed for a plane wave.

The attenuation length was also calculated in a broad wavelength interval (see Fig. 6) for smooth gold and silver films of thickness 47 nm, bordering glass and air in the Kretschmann–Raether geometry. These calculations were done by using the condition $|R^{-1}| \to 0$ for the reflection coefficient of Eqs. (1) and (2) (exact 0-order model) and also with formulas of Eqs. (5) and (6) (approximate 0-order model). The dielectric constants for gold and silver from [30–32] and for BK7 glass from [33] were used, as shown in Table 1. The calculated and experimental values of the attenuation length for 633 and 805 nm are also presented in Table 1.

As can be seen from Fig. 6, the attenuation length strongly increases with the optical wavelength, reaching values on the order of a millimeter at

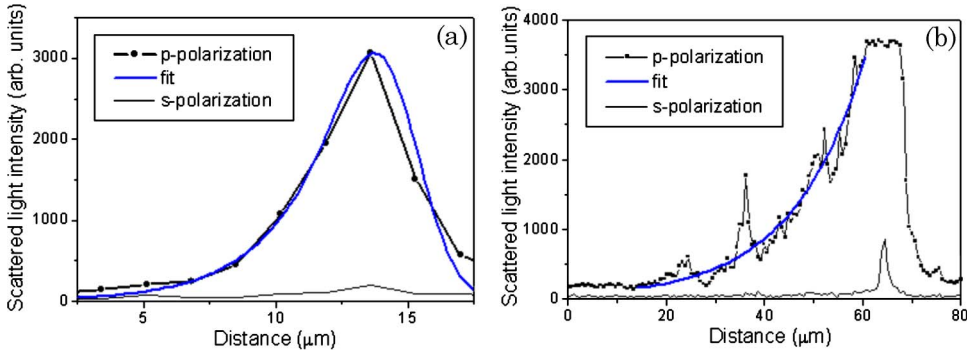

Fig. 4. (Color online) Measured distribution of the scattered light intensity near the laser illumination stripe for (a) 633 nm and (b) 805 nm.

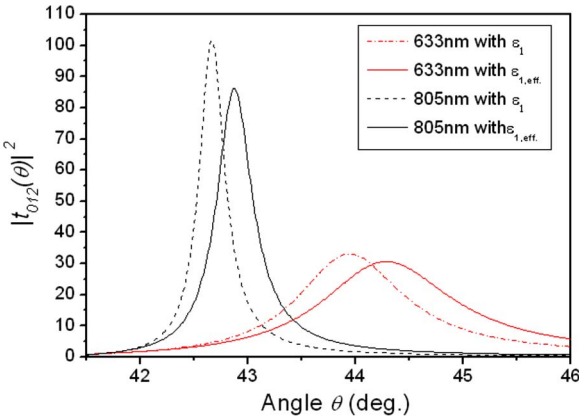

Fig. 5. (Color online) Dependence of the factor $|t_{012}(\theta)|^2$ on the angle for two wavelengths 633 and 805 nm, calculated for ε_1 from [30] and the corresponding effective dielectric constant of the gold film, $\varepsilon_{1,\mathrm{eff}}$.

$\lambda = 2.4\,\mu$m. The thickness of the film also strongly affects the SP losses. Figure 7(a) presents the angular dependences of the reflectivity, described by Eq. (1), in the vicinity of the resonance for different thicknesses of the gold film for an optical wavelength 633 nm. For thin films the resonance becomes very broad, while for thick films the dip in the reflectivity reduces, which means that the coupling of light with the SP mode decreases.

The dependence of the attenuation length on the thickness of the gold film [see Fig. 7(b)] shows that this length increases with the thickness of the film and experiences flattening of the dependence at larger thicknesses, which starts at around $d = 70$ nm.

5. Discussion

For observing the propagation of SPs, we used their scattering on the surface roughness, which is always present to a certain extent. Although the scattering of SPs was studied in many papers (see, for instance [15–19,26–29]), the question about the influence of the surface roughness on the propagation of SPs is still not completely understood, and the present paper is intended to contribute to answering this question. The calculations of the SP attenuation, based on the expressions for rescattering and conversion of SPs into light waves [16] give values for losses that are too low [29]. To estimate the influence of roughness, we followed [29], which described a quantitative model producing a good agreement with experimental observations. This model is an extension of previous theories [17,27,28].

As Fig. 2 and the values of $\varepsilon_{1,\mathrm{eff}}$ in Table 1 show, the roughness introduces noticeable changes for both studied wavelengths, 633 and 805 nm. Therefore, the determined attenuation lengths were also affected by the roughness. The surface roughness leads to an increase of the SP losses, which is reflected in the broadening of the SP resonance curve and the displacement of the resonance angle to larger angular values. Consequently, the dielectric constants of a metal obtained from the measurements of the SP resonance curves can be dependent on the surface roughness and also on internal inhomogeneities of the film that play a similar role. The measured roughness height $\delta \approx 2$ nm is still within the range of validity of the first-order approximation [34]. Calculated positive angular shifts and broadening of the resonance curves due to roughness are in qualitative agreement with conclusions of previous studies on the effect of roughness [19]. It should be noted that the reduction of the correlation length (provided that the averaged height of the roughness is the same) leads to an increase of the variations of the surface slope and also to a somewhat higher SP losses. The calculations for roughness parameters $\delta \le 0.5$ nm and $\sigma \ge 30$ nm show that the reduction of the attenuation length due to roughness is less than 2% for $\lambda \le 0.9\,\mu$m. This correction margin gradually increases with the optical wavelength to about 5% at $\lambda = 2.4\,\mu$m. An increase of the relative influence of roughness for longer wavelength can be explained as follows. Although with a longer wavelength the ratio δ/λ decreases, leading to a smaller contribution of roughness to attenuation, the reduction of the intrinsic losses in the metal owing to improved dielectric constants makes the relative role of roughness more important. When the influence of roughness is negligible, the attenuation length of SPs can be

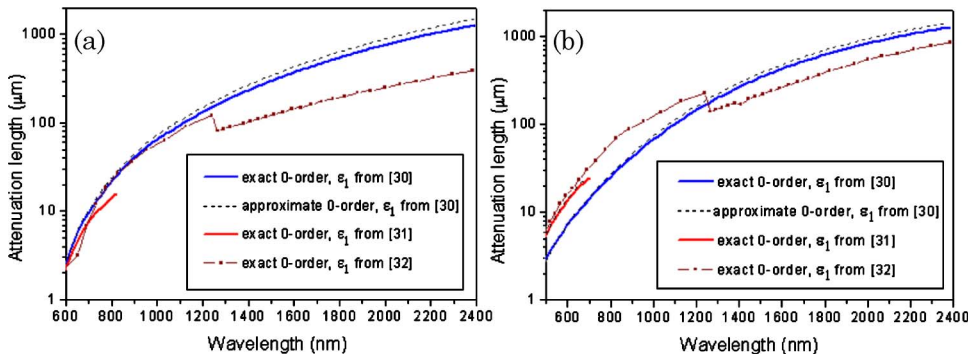

Fig. 6. (Color online) Surface plasmon attenuation lengths for (a) gold and (b) silver films of 47 nm thickness, calculated for a broad spectral range without account for roughness [the exact 0-order model, Eqs. (1) and (2); the results are shown by solid lines and solid lines with triangles] and approximate 0-order model [Eqs. (3)–(6) with $\Delta k_r = \Gamma_r = 0$; the results are shown by dashed lines]. The steps in the dependences, calculated with the data from [32], are due to the shifts present in this data.

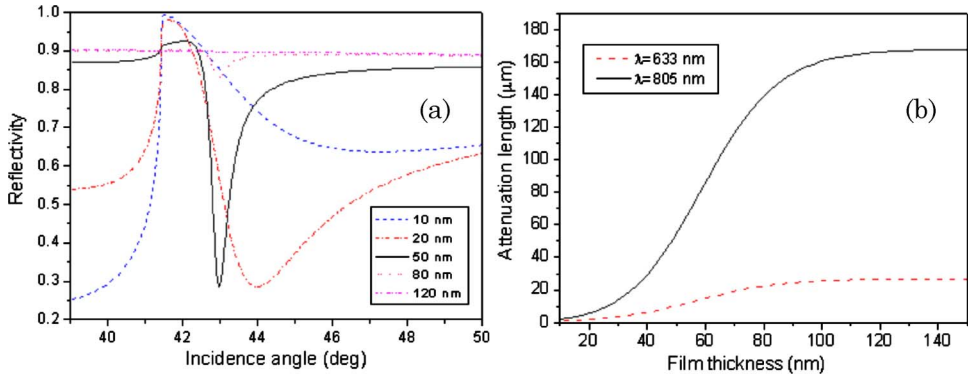

Fig. 7. (Color online) Influence of the thickness of the gold film on the properties of SPs: (a) SP resonance curves at 633 nm for different film thicknesses, (b) the dependence of the attenuation length on the film thickness for 633 and 805 nm. The dielectric constants from [30] are used.

calculated directly by applying the condition $|R^{-1}| \rightarrow 0$ to the reflection coefficient of light in Eq. (1).

The scattering on sub-wavelength-scale inhomogeneities has a broad and relatively smooth angular distribution [17], and measuring the distribution of the scattered light intensity along the direction of the SP propagation allows to infer the attenuation length L_{sp}. The presence of scratches and other inhomogeneities, such as grain boundaries, gives spikes in the scattered light and leads to additional attenuation of SPs.

The measurements of the widths of the SP resonance gives an alternative approach for the L_{sp} determination. In this case the focusing of light by a cylindrical lens produces a set of plane waves propagating within a certain angular interval. The light incident on the interface exactly at the resonance angle corresponds to the most efficient conversion of light into SPs, and therefore in the reflected light this area looks dark and corresponds to a dip in the intensity (see Fig. 2). Our results have demonstrated that both approaches, by a direct observation of the SPs attenuation and by measuring the SP resonance curve, give close values for the L_{sp} as presented in Table 1. For conditions similar to ours, the attenuation length at an optical wavelength of 800 nm was considered in [35], and a close value of 25 μm was obtained.

There are several applications of the obtained results. In particular, the knowledge of attenuation properties of SPs helps selecting the right wavelength for the SP microscopy [36]. Since the resolution in SP microscopy is determined by the attenuation length of the SPs, which is smaller for shorter wavelength, an employment of shorter optical wavelengths for the excitation of SPs is preferable for high-resolution microscopy. Attenuation characteristics of SPs are also important for direct [20,21] and ellipsometric [37] absorption spectroscopy with SPs. In these techniques it is desirable that attenuation of SPs due to metal is low, and this is achieved for longer optical wavelengths and the optimal and larger thicknesses of the metal film, although it should be noted that for thicker films the excitation efficiency of SPs is lower due to a reduction of the coupling of light with the surface plasmon mode.

6. Conclusions

In this work the attenuation length of SPs with a gold film at 633 and 805 nm was experimentally studied in the Kretschmann–Raether configuration by observing the distribution of the intensity of the scattered light. For a gold film of 47 nm thickness with roughness parameters $\delta = 2.0$ nm, and $\sigma = 36$ nm, we determined the SP attenuation length at 633 nm of 3.4 μm (the calculations with different sets of the dielectric constants for gold [30–32] produced values 2.5–3.6 μm) and at 805 nm this length was 15 μm (the theory gave values 11–17 μm). For comparison, the calculations of the attenuation length of SPs without accounting for roughness gave values 2.7–4.4 μm at 633 nm and 14–24 μm at 805 nm. The attenuation lengths were also determined from the widths of the angular dependences of the SP resonance and gave similar values of 3.0 μm for 633 nm and 17 μm for 805 nm. The roughness of the film was measured with an AFM, and the contribution of the roughness to the losses of SPs was evaluated, using the model for the SP resonance taking roughness into account. We proposed and implemented a procedure to calculate the effect of the surface roughness on the effective dielectric constant of the metal film. The SP attenuation length was also calculated for smooth gold and silver films in a broad optical spectral range, showing a strong increase of the propagation length with increasing optical wavelength. The coupling of light to the SP mode and the SP attenuation also strongly depends on the metal film thickness: the coupling is maximal for the optimal film thickness, and the losses strongly increase for thinner films.

We are thankful to Wonmuk Hwang for providing AFM for roughness measurements. This work was partially supported by the Robert A. Welch Foundation (grant A1546) and by the National Science Foundation (NSF) (grant 0722800).

References

1. R. W. Wood, "On a remarkable case of uneven distribution of light in a diffraction grating spectrum," Philos. Mag. **4**, 396–402 (1902).
2. U. Fano, "The theory of anomalous diffraction gratings and of quasi-stationary waves on metallic surfaces (Sommerfeld's waves)," J. Opt. Soc. Am. **31**, 213–221 (1941).
3. R. H. Ritchie, "Plasma losses by fast electrons in thin films," Phys. Rev. **106**, 874–881 (1957).
4. H. Raether and E. Kretschmann, "Radiative decay of non radiative surface plasmons excited by light," Z. Naturforsch. **23a**, 2135–2136 (1968).
5. E. Kretschmann, "Die bestimmung optischer konstanten von metallen durch anregung von oberflaechenplasmaschwingungen," Z. Phys. **241**, 313–324 (1971).
6. H. Raether, *Surface Plasmons on Smooth and Rough Surfaces and on Gratings* (Springer, 1988).
7. U. Jönsson, L. Fägerstam, B. Ivarsson, B. Johnsson, R. Karlsson, K. Lundh, S. Löfås, B. Persson, H. Roos, I. Rönnberg, S. Sjölander, E. Stenberg, R. Ståhlberg, C. Urbaniczky, H. Östlin, and M. Malmqvist, "Real-time biospecific interaction analysis using surface plasmon resonance and a sensor chip technology," BioTechniques **11**, 620–627 (1991).
8. C. E. Jordan, A. G. Frutos, A. J. Thiel, and R. M. Corn, "Surface plasmon resonance imaging measurements of DNA hybridization adsorption and streptavidin/DNA multilayer formation at chemically modified gold surfaces," Anal. Chem. **69**, 4939–4947 (1997).
9. A. V. Zayats, I. I. Smolyaninov, and A. A. Maradudin, "Nano-optics of surface plasmon polaritons," Phys. Rep. **408**, 131–314 (2005).
10. A. Degiron and D. R. Smith, "Numerical simulations of long-range plasmons," Opt. Express **14**, 1611–1625 (2006).
11. S. Negm and H. Talaat, "Surface plasmon resonance half-widths as measured using attenuated total reflection, forward scattering and photoacoustics," J. Phys. Condens. Matter **1**, 10201–10205 (1989).
12. A. Bouhelier and G. P. Wiederrecht, "Surface plasmon rainbow jets," Opt. Lett. **30**, 884–886 (2005).
13. H. Ditlbacher, J. R. Krenn, N. Felidj, B. Lamprecht, G. Schider, M. Salerno, A. Leitner, and F. R. Aussenegg, "Fluorescence imaging of surface plasmon fields," Appl. Phys. Lett. **80**, 404–405 (2002).
14. P. Dawson, F. de Fornel, and J-P. Goudonnet, "Imaging of surface plasmon propagation and edge interaction using a photon scanning tunneling microscope," Phys. Rev. Lett. **72**, 2927 (1994).
15. E. Kretschmann, "Decay of non radiative surface plasmons into light on rough silver films. Comparison of experimental and theoretical results," Opt. Commun. **6**, 185–187 (1972).
16. D. L. Mills, "Attenuation of surface polaritons by surface roughness," Phys. Rev. B **12**, 4036–4046 (1975).
17. E. Kretschmann, "The angular dependence and the polarization of light emitted by surface plasmons on metals due to roughness," Opt. Commun. **5**, 331–336 (1972).
18. A. A. Maradudin and D. L. Mills, "Scattering and absorption of electromagnetic radiation by a semi-infinite medium in the presence of surface roughness," Phys. Rev. B **11**, 1392–1415 (1975).
19. A. Hoffmann, Z. Lenkefi, and Z. Szentirmay, "Effect of roughness on surface plasmon scattering in gold films," J. Phys. Condens. Matter **10**, 5503–5513 (1998).
20. H. Kano and S. Kawata, "Surface-plasmon sensor for absorption-sensitivity enhancement," Appl. Opt. **33**, 5166–5170 (1994).
21. A. A. Kolomenskii, P. D. Gershon, and H. A. Schuessler, "Surface-plasmon resonance spectrometry and characterization of absorbing liquids," Appl. Opt. **39**, 3314–3320 (2000).
22. G. Kovacs, "Optical excitation of surface plasmon-polaritons in layered media," in *Electromagnetic Surface Modes*, A. D. Boardman, ed. (Wiley, 1982), pp. 143–197.
23. L. M. Brekhovskikh, *Waves in Layered Media*, 2nd ed. (Academic, 1980).
24. C. A. Ward, K. Bhasin, R. J. Bell, R. W. Alexander, and I. Tyler, "Multimedia dispersion relation for surface electromagnetic waves," J. Chem. Phys. **62**, 1674–1676 (1975).
25. P. Dawson, B. A. F. Puygranier, and J-P. Goudonnet, "Surface plasmon polariton propagation length: a direct comparison using photon scanning tunneling microscopy and attenuated total reflection," Phys. Rev. B **63**, 205410 (2001).
26. E. Kröger and E. Kretschmann, "Surface plasmon and polariton dispersion at rough boundaries," Phys. Stat. Sol. (B) **76**, 515–523 (1976).
27. F. Toigo, A. Marvin, V. Celli, and N. R. Hill, "Optical properties of rough surfaces: general theory and the small roughness limit," Phys. Rev. B **15**, 5618–5626 (1977).
28. S. O. Sari, D. K. Coben, and K. D. Scherkoske, "Study of surface plasma-wave reflectance and roughness-induced scattering in silver foils," Phys. Rev. B **21**, 2162–2174 (1980).
29. E. Fontana and R. H. Pantell, "Characterization of multilayer rough surfaces by use of surface-plasmon spectroscopy," Phys. Rev. B **37**, 3164–3182 (1988).
30. *American Institute of Physics Handbook*, D. E. Gray, ed. (McGraw-Hill, 1972), p. 105.
31. U. Schröder, "Der einfluss dünner metallischer deckschichten auf die dispersion von oberflaechenplasmaschwingungen in gold-silber-schichtsystemen," Surf. Sci. **102**, 118–130 (1981).
32. *Handbook of Optical Constants of Solids*, E. D. Palik, ed. (Academic, 1985).
33. *The Properties of Optical Glass*, H. Bach and N. Neuroth, eds. (Springer, 1995), pp. 4–9.
34. H. Raether, "The dispersion relation of surface plasmons on rough surfaces; a comment on roughness data," Surf. Sci. **125**, 624–634 (1983).
35. M. U. Gonzalez, J.-C. Weeber, A. L. Baudrion, A. Dereux, A. L. Stepanov, J. R. Krenn, E. Devaux, and T. W. Ebbesen, "Design, near-field characterization, and modeling of 45° surface-plasmon Bragg mirrors," Phys. Rev. B **73**, 155416 (2006).
36. W. Hickel, D. Kamp, and W. Knoll, "Surface-plasmon microscopy," Nature **339**, 186 (1989).
37. T. Iwata and S. Maeda, "Simulation of an absorption-based surface-plasmon resonance sensor by means of ellipsometry Appl. Opt. **46**, 1575–1582 (2007).